Crespo-Bardera, E., Garrido Martin, A., Fernandez-Duran, A. & Sanchez-Fernandez, M. (2020). Design and Analysis of Conformal Antenna for Future Public Safety Communications: Enabling Future Public Safety Communication Infrastructure. *IEEE Antennas and Propagation Magazine, 62*(4), 94–102.

DOI: 10.1109/map.2020.3000711

Design and Analysis of Conformal Antenna for Future Public Safety Communications

Estefanía Crespo-Bardera, Aarón Garrido Martín, Alfonso Fernández-Durán, Eva Rajo-Iglesias, Matilde Sánchez-Fernández

***Abstract*—Future 4G wireless communication systems include, in their capabilities portfolio, emergency specific needs such as data-support, broadband communication and extremely high reliability. An emergency situation can be addressed with undoubtedly more chances of success if augmented information is enabled within the public safety communication novel capabilities. For full augmented information provision based on broadband transmission, in this work a user end (UE) communication capabilities enhancement is addressed by deploying multiple antennas without compromising the first responder equipment portability and lightweight. With this aim, we propose the design of a 4.9 GHz conformal antenna array at the rescuer side (integrated in a helmet) and evaluate its performance in terms of relative data rate gain. The conformal array design is based on traditional patch antennas that take into account the need of being deployed over an ellipsoidal surface. The antenna array is simulated and then built and several parameter characterization (bandwidth, radiation pattern, reflection coefficient and mutual coupling) and measurements are undertaken in order to ensure the suitability of the design. Furthermore, an analysis of the specific absorption rate (SAR) is performed to guarantee that the exposure to electromagnetic fields is below the standardized levels.**

***Index Terms*—Conformal antenna, public safety, SAR, LTE.**

I. Introduction

Over the last decade (2006–2015), a total of 771, 911 people were killed in disasters (see Fig. 1). People directly affected by disasters, defined as the population requiring immediate assistance such as rescuing, basic survival needs, medical assistance and also those reported injured or homeless are close to 200 million people every year [1]. In such cases, technology and, in particular, communication and information systems are key instruments that have always played and will play a very important role on disaster managing, preparedness and intervention [2]–[4].

New trends in emergency communications to support first responders and public protection and disaster relief personnel aim for reliable broadband connectivity enabling augmented information services such as high-resolution images, thermal vision, augmented and/or virtual reality and cognition, video transmission or real-time high resolution maps [5], [6]. Network solutions within 4G wireless communication systems (LTE, LTE advanced-pro) [7], [8] are adding new features to make the mobile network capable of conveying critical communication services. Some general criteria that should be taken into consideration during the network design are: availability, security, robustness, user interoperability, reliability and optimized group communication. However, a full communication infrastructure may not be available in most disaster scenarios and challenges include not enough bandwidth to provide augmented information services or extremely limited wireless coverage, such as tunnels or caves.

Addressing either the challenge of broadband communication or the improvement of a limited wireless coverage scenario, future wireless technologies have widened the range of frequency bands to provide emergency services [9], [10], allowing other bands usage (e.g. 4.9 GHz, 2.6 GHz) and solving the propagation issue of very restricted frequency bands such as the exclusive 400 MHz or 700 MHz available for trunking services. Nevertheless, even in scenarios with large bandwidth available, the broadband transmission capability needed for full augmented information provision [11], [12], can only be achieved with multiple-input multiple-output (MIMO) antenna technology, being key that multiple antennas are deployed at both sides of the communication system, i.e. at the base station (BS) and at the user end (UE), in this application scenario the first responder or rescuer. The major challenge then to provide full MIMO is to be able to seamless deploy a large number of antennas in the user end [13] and it is done so by using the emergency personnel equipment, for example, the helmet.

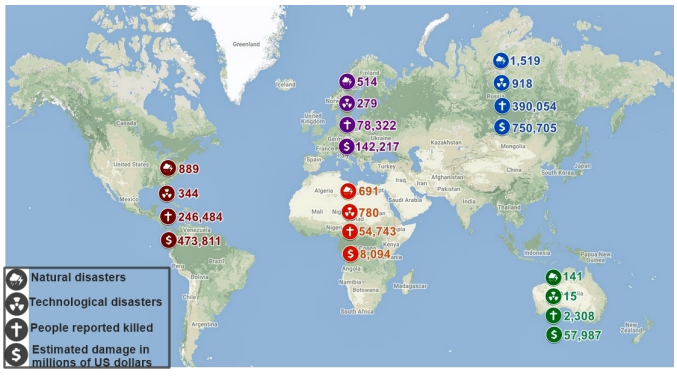

Fig. 1: Disaster figures for the decade 2006 – 2015 per continent. Data obtained from 2016 World Dissasters Red Cross report [1].

In this work, a conformal antenna array with $M = 4$ elements working in the 4.9 GHz public safety frequency band [14] is proposed. This antenna directly implemented on the user side will provide the rescuer with the benefits of MIMO technology, overcoming typical communication sce-

A. Garrido Martín and A. Fernández-Durán are with Nokia Spain, María Tubau 9, 28050 Madrid, Spain. E-mail: {aaron.garrido_martin.ext, alfonso.fernandez_duran}@nokia.com

E. Crespo-Bardera, E. Rajo-Iglesias and M. Sánchez-Fernández are with the Signal Theory & Communications Department, Universidad Carlos III de Madrid, Spain. E-mail: {ecrespo, eva, mati}@tsc.uc3m.es

This work has been partly funded by the Spanish Government through projects CIES (RTC-2015-4213-7), MIMOTEX (TEC2014-61776-EXP) and TERESA-ADA (TEC2017-90093-C3-2-R) (MINECO/AEI/FEDER, UE).

narios where the user end only has one or at the most two antennas. Additionally, a potential LTE network scenario to serve in emergency scenarios is shown and eventually consider a two-hop architecture based on relaying, to provide broadband services in scenarios with null or very low coverage. Finally, the proposed first responder communication device that integrates imaging, measurement and communication equipment is shown and the evaluation of the whole solution by providing the achieved throughputs in different bandwidth scenarios is performed. At this point, it is important to underline that the conformal antenna is designed to be part of a fully integrated solution. This fact takes this work a step further with respect to antenna proposals previously designed to be integrated onto helmets [15]–[17].

II. Conformal Antenna Design

The proposed antenna array, based on textile technology, is designed to be conformed on the cover of a safety helmet operating in the 4.9 GHz public safety frequency band.

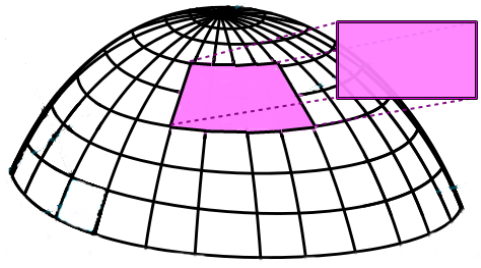

Fig. 2: Projection of a plane onto an ellipsoidal surface.

It should be noticed that the sole purpose of choosing textile technology for the conformal antenna design is for the ease and flexibility that this technology provides in the design of a proof–of–concept. Thus, the need of directly fabricating the antenna merged in the helmet material what could imply a long manufacturing time is avoided. All the design procedure detailed next could eventually applied to other technology.

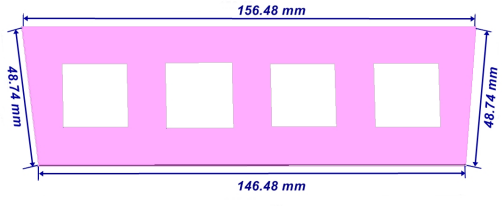

Fig. 3: Design of the proposed antenna.

The design methodology is mainly the same as that applied to design a traditional patch antenna with the exception that the effect of conforming the antenna should be counteracted to achieve the desired resonant frequency. With this in mind, we consider as simplest means of constructing the conformal antenna array, the design of a linear patch antenna array that is afterwards bent around an ellipsoidal surface (safety helmet) resulting in the desired conformed form. The planar geometry of the antenna is geared to show a rectangular form once conformed. For that purpose it was necessary to compensate

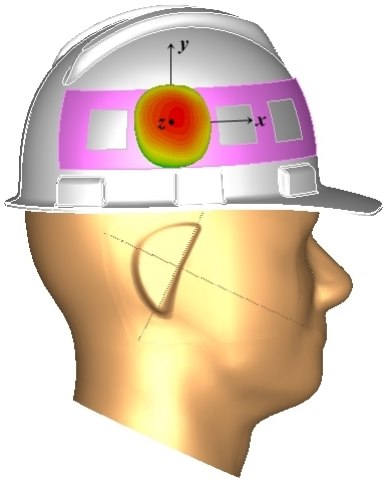

(a)

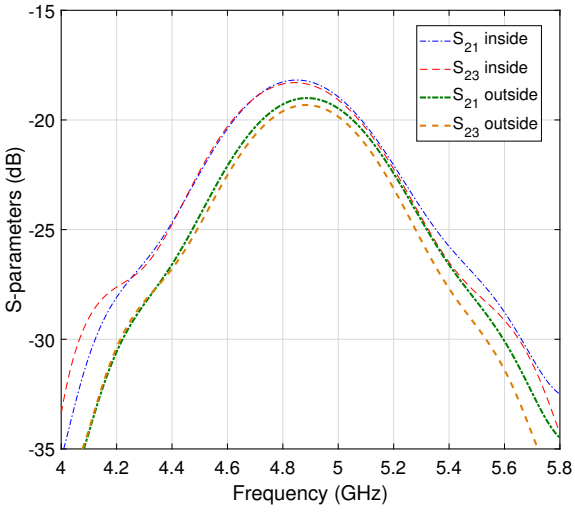

(b)

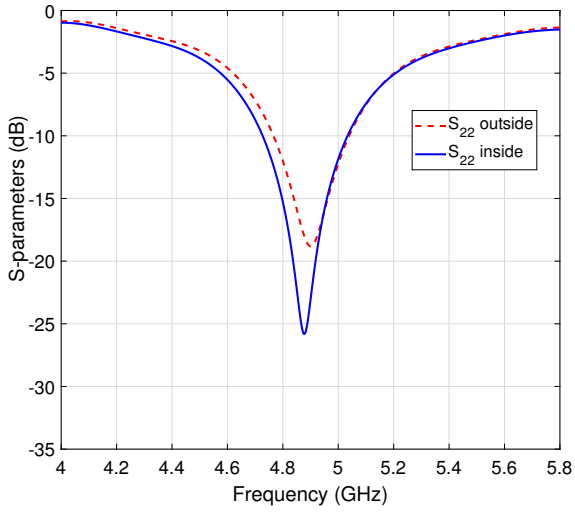

(c)

Fig. 4: Simulated performance: (a) Conformal antenna deployment over a safety helmet and radiation pattern for element placed approximately in the middle of the linear array; (b) Mutual coupling (S_{21} and S_{23}) with the two nearest antennas surrounding left and right, respectively and (c) Return losses (S_{22}).

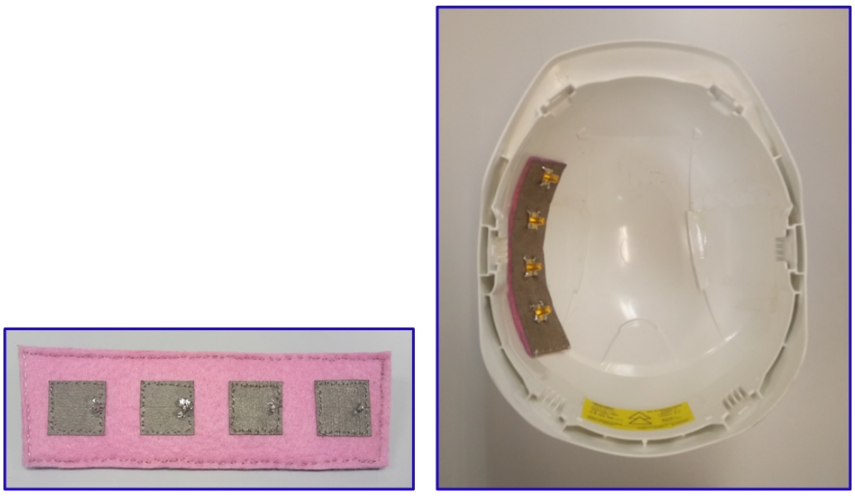

Fig. 5: The designed planar antenna and its conformed version inside a safety helmet.

the effect of projecting a plane onto an ellipsoid as shown in Fig.2.

The design of the proposed antenna with $M = 4$ elements linearly deployed was carried out using CST Microwave Studio (CST MWS). As substrate, common felt with thickness of 3 mm and dielectric constant of 1.38 was used, whilst the conductive part was developed with electro–textile material. For feeding, simple probe feeds with 50 Ohms impedance are used. Regarding the safety helmet, we deem that its rigid outer section known as shell, has a common thickness of 3 mm and it is made of thermoplastic material known as Acrylonitrile Butadiene Styrene (ABS) whose dielectric constant is $\epsilon_r = 3$. The dimensions considered for the helmet in the simulation are $225 \times 180 \times 130$ mm. Finally, the proposed conformal antenna is assumed to operate in close proximity to human head that will be modeled by a phantom.

The antenna initial design parameters (position of the feeding probes, patches sizes, distance among elements and thickness of the material used as substrate) had to be optimized to achieve minimum reflection coefficient at the desired working frequency, low mutual coupling (MC) and proper bandwidth. This optimization procedure has been necessary given that a shift of the resonance frequency was observed probably due to the bend effect and the presence of a lossy medium like the human tissue. Also, keeping in mind that this is an initial proof–of–concept the behavior of the antenna array both when it is conformed outside and inside the helmet has been also analyzed. The last alternative would eventually be the most suitable from a future industrialization point of view since the helmet may act as radome and also the helmet does not have to be modified or drilled, preserving its protecting properties.

The optimized parameters for the array geometry consist of a 35.77 mm inter-element distance ($\approx 0.6\lambda$) to minimize the MC among antennas. From the $M = 4$ squared patch antennas the two antennas in the middle of the array have side length 22.17 mm and the two antennas at the extremes of the array have side length 22.4 mm. The total planar array perimeter is equal to 400.44 mm (see Fig. 3).

For the optimized design parameters, simulated results are provided in terms of the antenna radiation patterns and S–parameters. The radiation patterns of the individual antennas slightly vary, giving rise to antenna gains going from 7.81 to 8.47 dB depending on the relative position of the radiating element and with negligible backward power levels which are under -20 dB. An example of the radiation pattern of one of the antennas is given in Fig.4.a. On the other hand, the simulated reflection coefficients of about -18.5 dB indicate that each individual antenna is well matched at the working frequency of 4.9 GHz. A low MC (S_{21} y S_{23} parameters) of -19 dB can be observed among radiating elements. A simulated bandwidth of 260 MHz (4.78 GHz - 5.04 GHz) is achieved.

A. *Experimental antenna characterization*

In order to verify the proposed design, an antenna prototype manually fabricated is presented in Fig.5. The design dimensions are the same as those previously described.

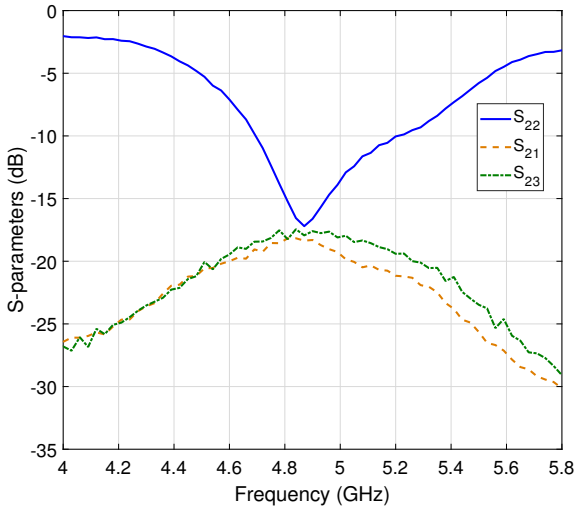

Fig. 6: Measured S–parameters for an element placed in the middle of the conformal array.

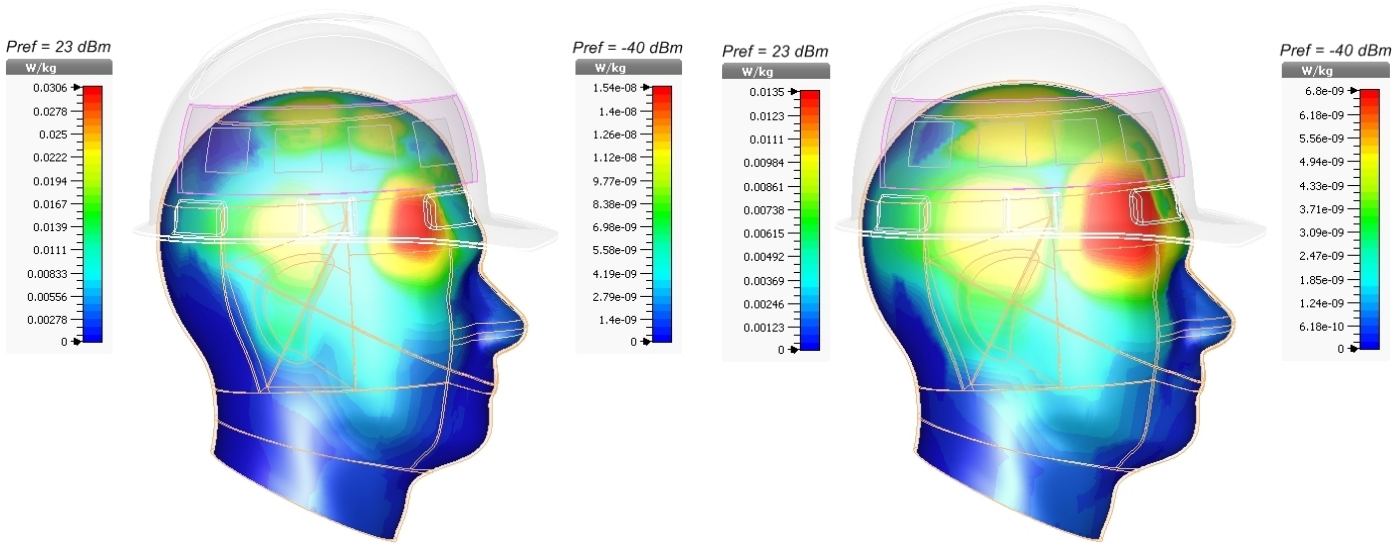

(a) Averaged over 1 g outside the helmet.

(b) Averaged over 10 g outside the helmet.

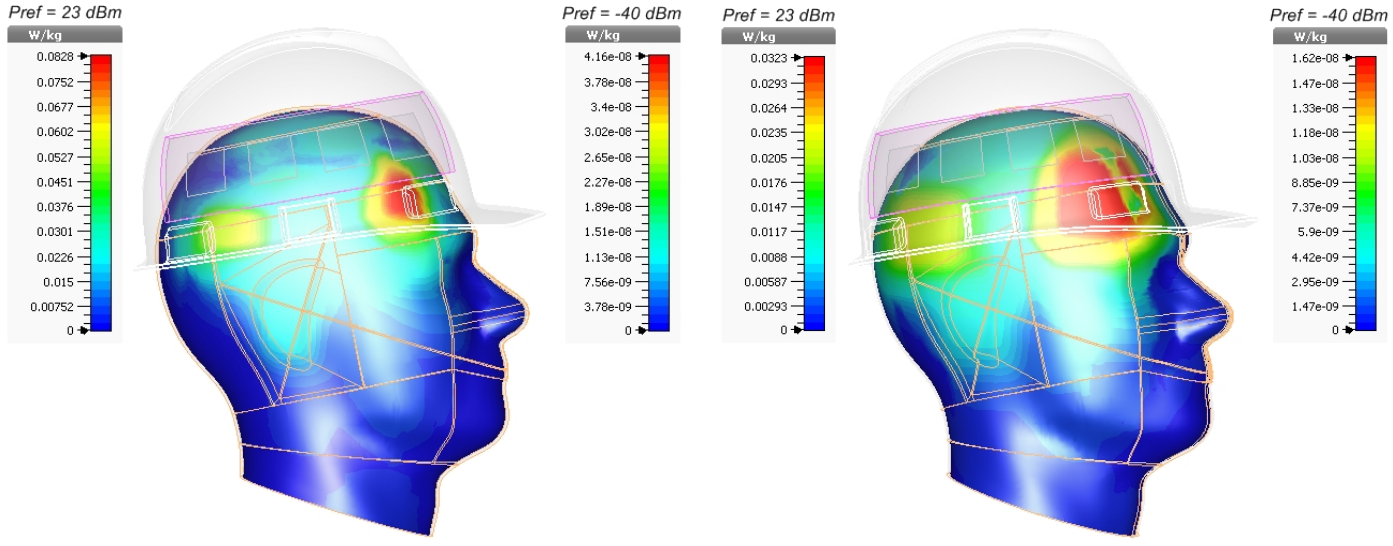

(c) Averaged over 1 g inside the helmet.

(d) Averaged over 10 g inside the helmet.

Fig. 7: SAR distribution averaged over 1 g and 10 g of tissue for different reference power values $P_{\text{ref}}(\text{dBm}) = \{-40, 23\}$ corresponding to the minimum and maximum transmitted power by a UE in LTE. Results are presented when the antenna is conformed outside and inside the helmet.

Fig. 6 shows the measured results of S–parameters. It can be observed that reasonable agreement is achieved between simulations (see Fig.4) and measurements. The measured return loss is better than -16 dB over the operating frequency band of 4.9 GHz. The measured bandwidth of the antenna extends from about 420 MHz. With respect to the MC, values below -17.5 dB have been measured. It should be noticed that the small disagreements might be mainly caused by manufacturing inaccuracies.

B. Specific absorption rate analysis

The deployment of a large number of antennas at the user side, always generates reservations due to its potential effect on the human body. Therefore, analyzing the energy which is absorbed by a biological tissue mass when it is exposed to a radio frequency electromagnetic field seems desirable during the design of an antenna for body-centric wireless communications. Specifically, the specific absorption rate (SAR) defined in (1), is a metric that allows us to measure that effect typically by averaging over the whole body or over a specific sample volume of biological tissue (generally 1 g or 10 g).

$$\text{SAR} = \frac{\sigma E^2}{2\rho} \qquad \text{(W/Kg)} \tag{1}$$

where σ is the tissue conductivity, E^2 represents the electric field strength and ρ is the tissue density.

Based on the foregoing, an evaluation of the electromagnetic energy absorbed by the human head when is located under the ground of the proposed 4.9 GHz conformal antenna is shown as follows. The SAR is computed in CST MWS using a phantom head model (SAM) that emulates the shell and liquid of a real human head and the IEEE C95.3 [18] averaging method. As reference input power, two different values are considered, 23 dBm and -40 dBm, established

as maximum and minimum transmitted power values for a LTE user equipment. Lastly, as baseline for comparison in the analysis we considered as safer limits for a partial body part the ones established in United States by the Federal Communications Commission (FCC) below 1.6 W/Kg for 1 g of tissue, and also the ones defined in the European Union by the European International Electro Technical Commission (IEC), that is, 2 W/Kg for 10 g of biological tissue volume.

Fig. 7 shows the SAR distribution when the proposed antenna is conformed inside and outside a helmet situated in a human head for the two reference input power values. The peak SAR values for the two different input power levels are summarized in Table I and Table II, respectively.

TABLE I: Simulated peak SAR values in W/Kg for $P_{\text{ref}} = -40$ dBm

	SAR Average over 1 g of tissue	SAR Average over 10 g of tissue
Outsite the helmet	$1.54e^{8}$	$6.8e^{9}$
Inside the helmet	$4.1e^{8}$	$1.62e^{8}$

TABLE II: Simulated peak SAR values in W/Kg for $P_{\text{ref}} = 23$ dBm

	SAR Average over 1 g of tissue	SAR Average over 10 g of tissue
Outsite the helmet	0.03	0.013
Inside the helmet	0.08	0.03

As expected, higher SAR values are obtained when the antenna is conformed inside the helmet due to the close proximity with the biological tissue. Despite that, the simulation results show acceptable SAR values satisfying the international standards. Finally, it is worth mentioning that the proposed conformal antenna achieves SAR levels in the same range than other antenna designs whose performance has also been studied in practical helmet models [15].

III. Technological Proposal for Future Public Safety Communications

The proposed network and physical layer solution seeks to reliably reach emergency locations with limited communication infrastructure and/or low coverage and at the same time to enable the provision of services based on augmented information. Such a solution is carried out by combining an LTE two-hop architecture based on relaying with an augmented information–enabled user communication device enhanced with the MIMO-based conformal antennas design described in Sec. II.

A. LTE-based network architecture

The proposed LTE-based network architecture distinguishes two main radio links (see Fig. 8). The first radio link is defined by the BS coverage area and reaches a relay node (RN), allowing this way a coverage extension without deploying a new fixed base station [19]. The second link is given by the RN coverage area and is defined between the RN and the

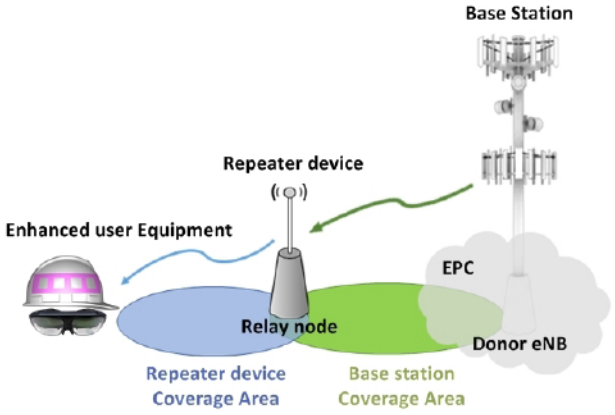

Fig. 8: Diagram of the LTE relaying network architecture.

enhanced user equipments (UE) which is not served directly by the E-UTRAN [8].

It should be noted that in order to provide the needed broadband capabilities for augmented information, this relaying architecture would need to implement MIMO technology end to end. LTE-advanced provides MIMO solutions for both the downlink and uplink, and MIMO relaying architectures used for IEEE 802.16m are applicable to LTE-advanced as described in [20].

B. AI–enabled user communication device

The proposed first responder communication device integrates not only specific communication equipment, but also imaging elements that will allow services based on augmented information. All these elements have been integrated in the proof–of–concept rescuer's helmet (see Fig. 9). Next, a short description of all the elements shown in Fig. 9 is provided:

1) *Smart-glasses with augmented-reality.* This element serves as interface between the first responder/rescuer and the available multimedia services. Different images can be projected for the first responder information, also images and videos can be recorded and sent to the support team.
2) *Power bank.* This element supplies energy to the whole system, excluding the smart glasses that have its own battery.
3) *Communications bridge unit (Raspberry Pi).* This element acts as a bridge between the smart-glasses and the rest of user equipment components.
4) *Thermal camera.* This component along with the smart-glasses provides thermal vision to first responders in poor visibility scenarios (e.g. fire scenarios full of smoke).
5) *LTE dongle.* This component enables the communication between the UE components and the LTE network. The LTE dongle should have as many antenna ports as individual antennas are included in the conformal design.
6) *Conformal antenna.* These radiating elements are developed directly at the user end via embedded textile technology allowing to take advantage of the benefits

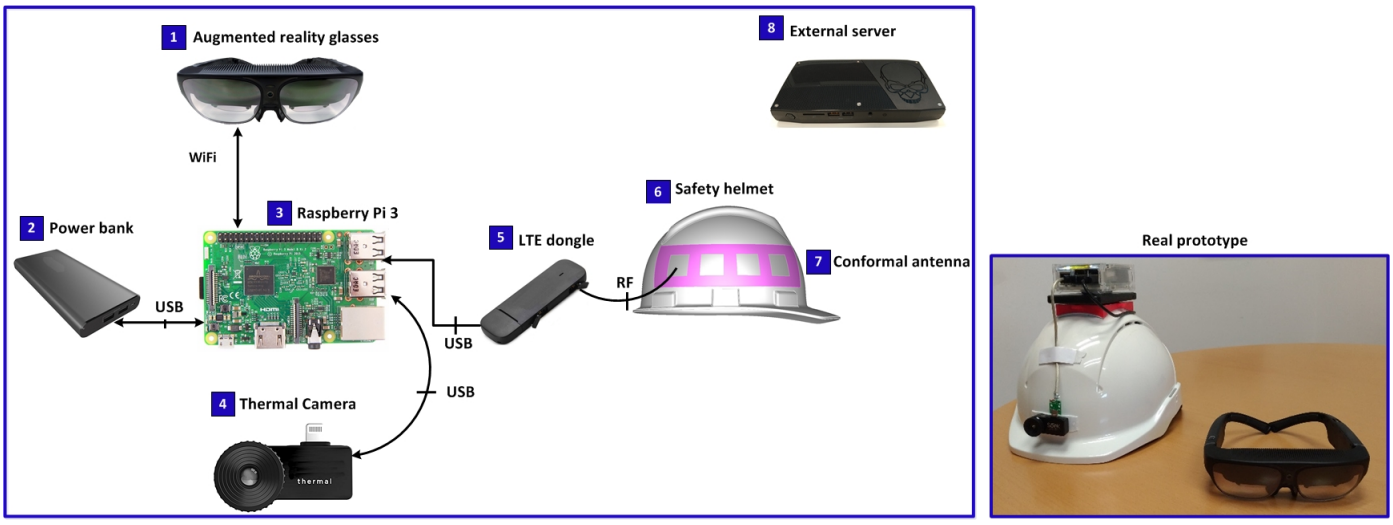

Fig. 9: Components of the proposed user equipment and its integration in a real prototype

offered by MIMO technology such as spectral efficiency improvement.

7) *Safety helmet.* All elements except the command and control center server described in 8) are envisioned to be mounted over the rescuers' helmet giving rise to an all-in-one AI–communication system.
8) *Command and control center server.* It is an external element conceived to supervise first responders interventions and that provides them practical real–time information.

C. Addressing AI throughput requirements

LTE-advanced allows 8×8 MIMO implementations in the downlink (i.e. 8 antennas in the BS and 8 antennas in the UE) and 4×4 MIMO in the uplink (4×4, i.e. 4 antennas in the UE and 4 antennas in the BS). In this work, the uplink throughput requirement is evaluated to show the benefits derived from the integration of the proposed conformal array into the user terminal. The focus is in the uplink, since undoubtedly it has the most restrictive performance, specifically, in the link between the UE and a MIMO–RN in the case of a low coverage scenario needing a two-hop architecture or between the UE and the multi–antenna BS for a one-hop architecture.

To obtain the uplink throughput gain, a metric is proposed, Δ_R, that allows us to measure the relative data rate gain in (bits/s) for a given bandwidth W in Hz when comparing a single-antenna UE whose propagation scenario is characterized by the channel matrix $\mathbf{H}_{\text{SIMO}}$ with a multiple antenna UE using the channel $\mathbf{H}_{\text{MIMO}}$. The gain is computed by getting the enhanced UE throughput with respect to that obtained by a single-antenna UE when the transmitted power is the same and there is no channel knowledge available. The general expression is given by

$$\Delta_R = W \log_2 \left[\frac{\det\left(\mathbf{I}_N + \frac{\mathsf{SNR}}{M}\mathbf{H}_{\text{MIMO}}\mathbf{H}_{\text{MIMO}}{}^{\dagger}\right)}{\det\left(\mathbf{I}_N + \mathsf{SNR}\mathbf{H}_{\text{SIMO}}\mathbf{H}_{\text{SIMO}}{}^{\dagger}\right)} \right] \tag{2}$$

where SNR represents the signal–to–noise ratio, $\mathbf{I}_N$ is the $N \times N$ identity matrix and $\mathbf{H}_{\text{MIMO}}$, $\mathbf{H}_{\text{SIMO}}$ denote the narrowband MIMO $N \times M$ and SIMO (single-input multiple-output) $N \times 1$ channel matrices, respectively. It must be noticed that M is the number of antennas at the UE and N at the RN/BS.

In order to provide a realistic channel model to be applied in (2), that takes into account the conformal antenna design parameters (mutual coupling, radiation patterns, etc.) and geometry, the channel matrix between the UE and the RN/BS is generated following the model provided in [21]:

$$\mathbf{H}_{\text{MIMO/SIMO}} = \mathbf{C}_N \mathbf{B}_N^{\dagger} \mathbf{S} \mathbf{B}_M \mathbf{C}_M \tag{3}$$

$\mathbf{C}_N$ is an $N \times N$ matrix and $\mathbf{C}_M$ an $M \times M$ matrix representing the mutual coupling in reception and transmission. $\mathbf{B}_M$ and $\mathbf{B}_N$ given by (4), (5) are the $N \times L'$ and $L \times M$ receive and transmit beamforming rectangular matrices that depend on the antenna geometry defined by the m-th antenna position $\mathbf{r}_m$ in the transmitter and the n-th antenna position $\mathbf{r}'_n$ at the receiver and the plane waves' receiving and emitting directions ($\mathbf{k}'_{l'}$ and $\mathbf{k}_l$). Finally, $\mathcal{G}_m(\theta, \phi)$ is the m-th transmit antenna radiation pattern and $\mathcal{G}'_n(\theta', \phi'))$ is the n-th receive antenna radiation pattern, characterized both in azimuth (ϕ) and elevation (θ).

$$\mathbf{B}_M = \begin{bmatrix} \mathcal{G}_1(\theta_1, \phi_1) e^{-j\mathbf{k}_1 \cdot \mathbf{r}_1} & \dots & \mathcal{G}_M(\theta_L, \phi_L) e^{-j\mathbf{k}_1 \cdot \mathbf{r}_M} \\ \vdots & \ddots & \vdots \\ \mathcal{G}_1(\theta_1, \phi_1) e^{-j\mathbf{k}_L \cdot \mathbf{r}_1} & \dots & \mathcal{G}_M(\theta_L, \phi_L) e^{-j\mathbf{k}_L \cdot \mathbf{r}_M} \end{bmatrix} \tag{4}$$

$$\mathbf{B}_N = \begin{bmatrix} \mathcal{G}_1(\theta'_1, \phi'_1) e^{j\mathbf{k}'_1 \cdot \mathbf{r}'_1} & \dots & \mathcal{G}_1(\theta'_L, \phi'_L) e^{j\mathbf{k}'_L \cdot \mathbf{r}'_1} \\ \vdots & \ddots & \vdots \\ \mathcal{G}_N(\theta'_1, \phi'_1) e^{j\mathbf{k}'_1 \cdot \mathbf{r}'_N} & \dots & \mathcal{G}_N(\theta'_L, \phi'_L) e^{j\mathbf{k}'_L \cdot \mathbf{r}'_N} \end{bmatrix} \tag{5}$$

Finally, $\mathbf{S}$ shown in (6), is a $L' \times L$ rectangular matrix that represents the channel discrete scattering function in the different propagation directions.

$$\mathbf{S} = \begin{bmatrix} S(\mathbf{k}'_1, \mathbf{k}_1) & \dots & S(\mathbf{k}'_1, \mathbf{k}_L) \\ \vdots & \ddots & \vdots \\ S(\mathbf{k}'_{L'}, \mathbf{k}_1) & \dots & S(\mathbf{k}'_{L'}, \mathbf{k}_L) \end{bmatrix} \quad (6)$$

With this channel model, the performance of the proposed conformal antenna integrated in the AI-communication device when $M = 4$ antennas are deployed in the helmet and when the BS is integrated by $N = \{4, 8\}$ antennas is evaluated. This evaluation scenario expands the typical LTE-advanced uplink MIMO scenario, where the BS would only have $N = 4$ antennas as mentioned at the beginning of this section. A total of 500 channel realizations are generated based on the channel model described in (3) and the antenna design parameters obtained above. Specifically, for the beamforming matrix ($\mathbf{B}_M$ in (4)) corresponding to the UE side where the conformal antenna array is deployed, the geometry assumes an inter-element distance of ($\approx 0.6\lambda$) to define the antenna positions $\mathbf{r}_m$, and the simulated radiation patterns that are depicted in Fig. 4(a) are used for $\mathcal{G}_m(\theta, \phi)$. Concerning the mutual coupling, despite it could have been neglected, the values obtained around -19 dB are considered. Finally, to characterize the scattering function at the transmitter side, full angular dispersion that is uniformly modeled is assumed. At the BS side for simplicity, ideal antennas without mutual coupling and omnidirectional radiation patterns are considered. With respect to the characterization of the scattering function at the receiver side, it is taken into consideration that the angular spread may be smaller than at the transmitter side. Then, it is assumed negligible angular spread in elevation and a narrow angular spread in azimuth of approximately 30°, trying to get a worst case performance. To define the receiving antenna positions $\mathbf{r}'_n$, a linear array integrated by N antennas with inter-element distance of $\lambda/2$ is considered.

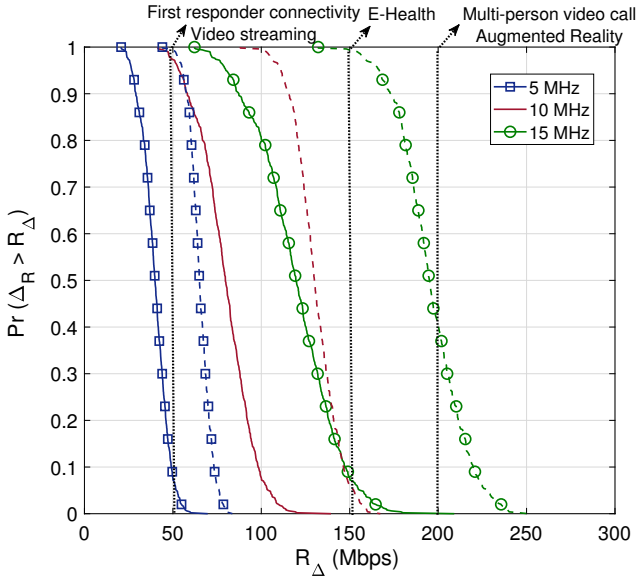

Fig. 10: CCDF of the relative data rate gain according to several bandwidth scenarios envisaged by broadband standards, $W = \{5, 10, 15\}$ when different antenna configurations are available at the RN/BS $N = 4$ (continuous line); $N = 8$ (dashed line). The CCDF represents the probability that a certain gain value R_Δ is achieved.

In order to study the data rate gains obtained when using one single antenna ($M = 1$) or several conformed antennas ($M > 1$) in the UE, we apply (2) with $\mathbf{H}_{\text{MIMO}}$ and $\mathbf{H}_{\text{SIMO}}$ generated following the aforementioned procedure. In Fig.10, the CCDF of the data rate gains assuming a specific SNR value of 15 dB is provided. In this scenario, we can get up rate gains from 35 Mbps up to 130 Mbps or from 40 Mbps up to 200 Mbps depending on the available MIMO scenario with respect to the corresponding SIMO scenario. These data rate gains may lead to improve emergency communications allowing the use of multimedia services like real-time video streaming, E-health or augmented reality [22]. The enabled services are shown in Fig. 10, where the vertical grey lines identify the required rates to achieve the different services. For example, in order to provide Multi–person video call or augmented reality, it would be necessary that the data rates are higher than 200 Mbps. Given that for 40% of the channel realizations, a rate gain larger than 200 Mbps is achieved, we can assure that deploying the conformal array antenna, these services can be provided with high probability.

IV. Conclusions

This work presents the design of a conformal antenna for public safety communications operating at 4.9 GHz. Being part of an improved user equipment proposal, the conformal antenna with $M = 4$ elements is directly developed at the rescuer end, concretely it is conceived to be embedded over a safety helmet allowing in this way to take advantage of the MIMO technology benefits (e.g. spectral efficiency improvement). Simulation and experimental results illustrate the feasibility of the proposed design such as suitable gain and reduced back radiation level, proper bandwidth, negligible mutual coupling and SAR values below the standardized levels. Regarding the data rate gain, we show that a user terminal equipped with our conformal antenna compared to one integrated by a single antenna, can reach gains in the range of 35 to 200 Mbps enabling the use of future 5G multimedia services during emergency situations. Bearing this in mind, we believe that the proposed antenna design is practical and can provide a significant opportunity for LTE-based next generation public safety communications.

References

[1] D. Sanderson and A. Sharma, *World Disasters Report. Resilience: saving lives today, investing for tomorrow*. International Federation of Red Cross and Red Crescent Societies, 2016.

[2] I. Kamen, "A new approach to disaster communication and control systems," *Electrical Engineering*, vol. 81, pp. 535–541, July 1962.

[3] T. C. Chan, J. Killeen, W. Griswold, and L. Lenert, "Information technology and emergency medical care during disasters," *Academic Emergency Medicine*, vol. 11, no. 11, pp. 1229–1236, 2004.

[4] R. Shaw, T. Izumi, and P. Shi, "Perspectives of science and technology in disaster risk reduction of Asia," *International Journal of Disaster Risk Science*, vol. 7, pp. 329–342, Dec 2016.

[5] N. Herscovici, C. Christodoulou, E. Kyriacou, M. S. Pattichis, C. S. Pattichis, A. Panayides, and A. Pitsillides, "m-health e-emergency systems: Current status and future directions [wireless corner]," *IEEE Antennas and Propagation Magazine*, vol. 49, pp. 216–231, Feb 2007.

[6] A. R. McGee, M. Coutire, and M. E. Palamara, "Public safety network security considerations," *Bell Labs Technical Journal*, vol. 17, pp. 79–86, December 2012.

[7] T. Doumi, M. F. Dolan, S. Tatesh, A. Casati, G. Tsirtsis, K. Anchan, and D. Flore, "LTE for public safety networks," *IEEE Communications Magazine*, vol. 51, pp. 106–112, February 2013.
[8] 3GPP TS 22.346, *"Isolated Evolved Universal Terrestrial Radio Access Network (E-UTRAN) operation for public safety; Stage 1"*, July 2018. V15.0.0.
[9] D. W. Matolak, K. A. Remley, C. Gentile, C. L. Holloway, Q. Wu, and Q. Zhang, "Peer-to-peer urban channel characteristics for two public-safety frequency bands," *IEEE Antennas and Propagation Magazine*, vol. 56, pp. 101–115, Oct 2014.
[10] A. Kumbhar, F. Koohifar, I. Güvenç, and B. Mueller, "A survey on legacy and emerging technologies for public safety communications," *IEEE Communications Surveys Tutorials*, vol. 19, no. 1, pp. 97–124, 2017.
[11] GreenTouch Application Taxonomy Project, "Greentouch application taxonomy," tech. rep., GreenTouch, Feb. 2012.
[12] J. Orlosky, K. Kiyokawa, and H. Takemura, "Virtual and Augmented Reality on the 5G Highway," *Journal of Information Processing*, vol. 25, pp. 133–141, 2017.
[13] M. Sánchez-Fernández, A. Tulino, E. Rajo-Iglesias, J. Llorca, and A. G. Armada, "Blended Antenna Wearables for an Unconstrained Mobile Experience," *IEEE Communications Magazine*, vol. 55, pp. 160–168, April 2017.
[14] F. C. Commission, "FCC 02-47," 2002. https://www.fcc.gov/auction/n3.
[15] Y. F. Cao, X. Y. Zhang, and T. Mo, "Low-Profile Conical-Pattern Slot Antenna With Wideband Performance Using Artificial Magnetic Conductors," *IEEE Transactions on Antennas and Propagation*, 2018.
[16] N. Nguyen-Trong, A. Piotrowski, T. Kaufmann, and C. Fumeaux, "Low-profile wideband monopolar uhf antennas for integration onto vehicles and helmets," *IEEE Transactions on Antennas and Propagation*, vol. 64, no. 6, pp. 2562–2568, 2016.
[17] S. L. Cotton, W. G. Scanlon, and J. Guy, "The κ-μ distribution applied to the analysis of fading in body to body communication channels for fire and rescue personnel," *IEEE Antennas and Wireless Propagation Letters*, vol. 7, no. 1, pp. 66–69, 2008.
[18] "IEEE Recommended Practice for Measurements and Computations of Radio Frequency Electromagnetic Fields With Respect to Human Exposure to Such Fields,100 kHz-300 GHz," *IEEE Std C95.3-2002*, 2002.
[19] 3GPP TS 36.300, *"Evolved Universal Terrestrial Radio Access (E-UTRA) and Evolved Universal Terrestrial Radio Access Network (E-UTRAN); Overall description; Stage 2"*, July 2018. V15.2.0.
[20] S. W. Peters, A. Y. Panah, K. T. Truong, and R. W. Heath, "Relay architectures for 3GPP LTE-advanced," *EURASIP Journal on Wireless Communications and Networking*, vol. 2009, p. 618787, Jul 2009.
[21] M. Sanchez-Fernandez, E. Rajo-Iglesias, O. Quevedo-Teruel, and M. L. Pablo-Gonzalez, "Spectral efficiency in MIMO systems using space and pattern diversities under compactness constraints," *IEEE Transactions on Vehicular Technology*, vol. 57, no. 3, pp. 1637–1645, 2008.
[22] E. Commission, *Communication from the Commission to the European Parliament, the Council, the European Economic and Social Committee and the Committee of the Regions. Connectivity for a competitive digital single market - Towards a European gigabit society.* Brussels, COM (2016) 587 Final.

Estefanía Crespo-Bardera (ecrespo@tsc.uc3m.es) is a Ph.D. student at Signal Theory and Communications Department of the Universidad Carlos III de Madrid. Her main research interests include MIMO technology, antenna design and RF channel modeling for wireless communications.

Aarón Garrido Martín (aaron.garrido_martin.ext@nokia.com) is a Research Engineer and an Integration Professional at Nokia Madrid, Spain. He received the B.E. degree in Telecommunications from Universidad Carlos III de Madrid.

Alfonso Fernández-Durán (Alfonso.fernandez_duran@nokia.com) Corporate Strategy Manager for Fixed Networks at NOKIA Madrid. He received a Master degree in Telecommunications engineering and a Ph.D. from Universidad Politécnica de Madrid.

Eva Rajo-Iglesias (eva@tsc.uc3m.es) Full professor at Universidad Carlos III of Madrid. Her current research interests include microstrip patch antennas and arrays, metamaterials, artificial surfaces and periodic structures, gap waveguide technology, MIMO systems, and optimization methods applied to electromagnetism.

Matilde Sánchez-Fernández (mati@tsc.uc3m.es) Associate professor at Universidad Carlos III of Madrid. Her current research interests are signal processing for wireless communications, MIMO techniques, channel modeling in wireless communications and game theory and machine learning techniques applied to communications.